Modification of Cellulose Nanofibers by ZnO Nanoparticles for Gas Sensing

Modification of Cellulose Nanofibers by ZnO Nanoparticles for Gas Sensing

Mazin A. Alalousi*, Yusra M. Al-Obaidi , Mustafa G. Jehad

University of Anbar, Collage of Science

mazin_alalousi@uoanbar.edu.iq

Abstract. Nanocellulose crystals (NCC) were isolated from the palm fronds by sonication and hydrolyzed processes and modification of them by the prepared ZnO nanoparticles (ZNPs) utilizes pulsed laser ablation in water. NCC:ZNPs layers were fabricated using the spin coating technique. The morphological properties of NCCs and NCC: ZNPs layers were investigated by atomic force microscopy (AFM), scanning electron microscopy and field-effect scanning electron microscope (FESEM) respectively. NCC fibers have been shown a long fibrous shape with layer fibrous sheets about 60 nm of thickness consist of nano tapes between 30 nm to 70 nm of width and thickness sequentially. ZNPs clusters appeared clearly in FE-SEM image as individual growths between 20 nm to 240 nm of size and around NCC fibers. The structural properties of prepared layers have been characterized by X-ray diffraction (XRD) technique, the domain peak of cellulose is found at 22.54^{o} mostly. There is increasing in the crystallinity indices with the number of layers were increased in both NCC and NCC: ZNPs films. The sensing of N_2, H_2 and NH_3 gases were measured, generally the sensitivity of gases increased with adding of ZNPs expect N_2.

Keywords. Nanocellulose crystals, ZnO nanoparticles, spin coating, Gas sensors.

1. Introduction

Cellulose is one of major, wide spread, and affordable biopolymer on Earth and global economic importance [1]. Recently, several studies have addressed different applications of different inorganic composites are formed based on cellulose fibers(NCCs) [2], new field emerges to use this promising material in electronics applications such as solar cells, gas sensing, biosensing, photodetecting, energy devices [3], and electrodes [4]. Cellulose fibers are found in nature as nano fibril-network with diameters from 100nm to one micrometer [5]. NCC depend on the used synthesis method. Due to their surface/volume ratio of cylindrical shape, asymmetric structure, high strength, low thermal expansion, and stiffness make the cellulose nanofibers (CNF) thin films are suitable for use in the sensing devices[2, 4]. Enhancement of the chemical sensing and performance gas sensing of cellulose has been confirmed by add several materials such as zinc oxide (ZnO)[6], titanium dioxide (TiO_2) [7], iron(III) oxide (Fe_2O_3)[8], Zirconium oxide (ZrO_2), cupric oxides (Cu_2O and CuO)[9], and graphen oxide (GO) [10]. Among the healthy metal oxide and stable in to harsh conditions is ZnO[11]. ZnO is a semiconductor with bandgap (3.37-3.47) eV, e-h binding energy (60 meV) [12, 13]. There have been many attempts to wrap cellulose fibers which are based on the curing process or the ultrasonic irradiation [14]. Polymer

unit of cellulose is $\beta - (1 => 4) - D - glucopyranose$ [15], which is likely to help bind zinc ions and consider them as nuclei for binding to fibers, as illustrated in figure (1)

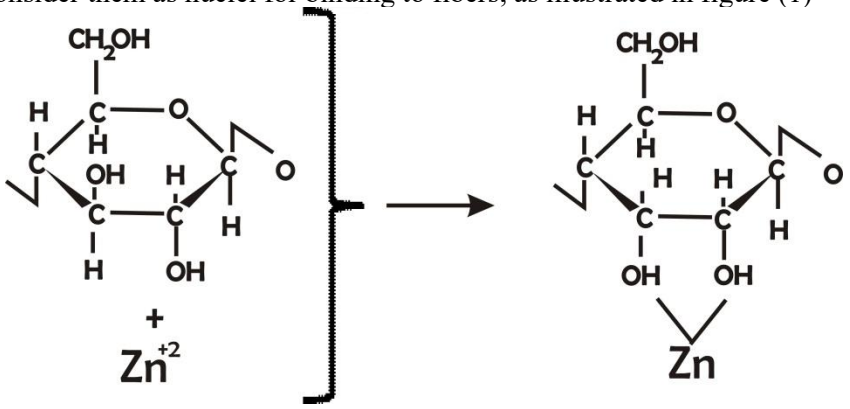

Figure 1. Likely correlation zinc with cellulose

Several metal oxide n-type semiconductors was reported for gas sensing include ZnO nanoparticles. These materials usually have a high operation temperature (100 – 400) ºC, but at the structural complication expense[8].

Toxic gases such as nitrogen (N_2)[16], hydrogen (H_2) and ammonia (NH_3)[17] are different in their toxic effects on human, when increase of their ratio. Nitrogen is a component of the breathed air. High increase of its ratio is not caused death due to oxygen displacement in the atmosphere[16]. But in general, its lack causes temporary ill-health if it continues beyond the normal time [18]. Therefore, it is necessary to have sensors in industrial areas where this type of gas is likely to leak abnormally. Flammable and explosive of hydrogen make it so dangerous[19]. Also ammonia is highly toxic gas with 50 ppm of concentration, it uses in wide industrial fields such as, foodstuffs, freezing, paper product[20]. Due to the danger of these gases, should be monitored in the places expected to be present using a affordable, reliable, low power consuming, highly sensitive, and small size gas sensor is the most candidate to work under unexpected conditions caused by toxic and explosive gases[21].

Generally, ZnO nanostructures or microstructures rarely used individually as gas sensors for N_2, H_2 and NH_3. Especially for N_2 due to the stability of N_2 that has a triple bond[22], and the weak adsorption for a chemically inert[23], except for the modification cases by adding ZnO structures to inorganic or organic combinations to impart some chemical and physical improvements. Among these biopolymers is cellulose Adsorption of these gases by cellulose can be demonstrate based on the dangling bond model[24].

Many studies are reported based on cellulose fibers, ZnO nanostructure, and their modification as gas sensors. Mani et al.[8] (2013) reported a sensor fabricated of ZnO thin films by spray pyrolysis technique. The observed film has a good selectivity to NH3 and short the response and recovery times (20 and 25) s. Hsia and Siaugluo[25] (2014) have been deposited pour ZnO by a rapid process of aerosol technique to detect CO gas at 110ºC to 180ºC of the operating temperature, with 100 ppm to 1000 ppm of concentration. They pointed to increase of sensitivity and decrease of response time with increase of the concentration and the operating temperature. Ebrahimials and Zakaria [24] (2016) synthesized Ppy/CS/ZnO nanospheres as a gas sensor for CO_2, N_2 and H_2. They found the sensitivity of H_2 was better than both CO_2 and N_2. Patil et al. (2016) [17] prepared PANI/ZnO thin films as a gas sensor for H2 and NH3, they confirmed that the sensitivity of films depended on thickness, grain size and surface morphology. Hang et al. [10](2018) prepared collections of sensors based on ZnO for sensing group of gases include NH_3 and N_2 with 100 ppm, the sensitivity of NH_3 and N_2 was less compere with selectivity of H_2S, also ZnO/SnO4 films showed a better performance compere ZnO films. Also, cellulose/ZnO nanocomposites were synthesized and studied for biosensing and antibacterial applications.

1.1. Sensing Mechanisms

The most common thesis to explain the sensing of gases depends on adsorption of atmospheric oxygen which is adsorbed by surface of ZnO with two modes;

$$O_2 + 2e^- \rightleftharpoons 2O^-(ads.)$$
$$O_2 + e^- \rightleftharpoons O_2^-(ads.)$$

Generally, all reducing gases are involved, depending on the surface adsorption of atmospheric oxygen and are adsorbed by it. Molecules of H_2 are adsorbed on the ZnO surface as protons and desorbed as water vapour as shown in following[22].

$$H_2 \rightleftharpoons 2H^+ + 2e^-$$

Same mechanism occurs with NH_3 depending on the probability of indirect adsorption [7];

$4NH_3 + O_2^- \rightleftharpoons 2H_2O + e^-$,

or $NH_3(gas) + O_2^- \rightleftharpoons NH_3(ads)$

The electron extracts from the conduction band which leads to increase the electrical resistance of the semiconductor. Another scenario can be found with cellulose fibers, during the polymerization between ZNPs and cellulose fibers, P-N hetrojuncton may be generated. Therefore, the gases adsorbed effects on the thickness of the depletion zone which lead to change in the electrical resistance of layers[26].

2. Experimental Part

2.1. Materials and reagents

Nanocellulose fibers have been synthesized by sonication and hydrolyzed processes as described in previous work[27]. Palm fronds were collected cut to small pieces with lengths 1-2 cm, dried and crushed to fine powder passing through a sieve 25 micron. The fine powder was treated with 1% sodium hydroxide, bleached with Sodium hypochlorite, washed and dried. The sample has been hydrolyzed with sulfuric acid at a concentration of 45% using strong stirring. The acidity was neutralized by washing the sample with distilled water several times. The suspension was filtered and treated with an ultrasonic device (Sono-plus HD 2070) for *120* minutes. Nanocellulose was collected, filtered, dried and converted to a fine powder.

The prepared cellulose fibers and ZnO powder (supplied by sigma-Aldrich-205532, $< 5\mu m$, 99.9% purity) were compressed by $10\frac{GN}{m^2}$ each separately for 24h to pellet.

ZnO nanoparticles were prepared by pulsed laser ablation technique using Nd-YAG pulsed laser ($\lambda = 1064\ \text{nm}, 100\text{mJ}, 10\text{ns}, 6\text{Hz}$) as wavelength, power, width, and duration of pulse respectively. ZnO pellet was immersed in double deionized water (DDDW) at depth 8mm. The concentration of the resulted colloid was 1530 ppm. Cellulose pellet was crushed using sandpaper ((JB-5) AA180 Aluminum oxide) and sift using sieve Vibratory Sieve Shaker (with mesh$50\mu m$). Two grams of CF powder have been mixed with 20 ml of DDDW using magnetic stirrer for 1h and continues heat at 100°C. The prepared solution was divided to two parts each one was 10ml. Then 10% Vol. of ZnONPs colloid was added in the same conditions to one of these. After that the mixes have been left for 72h in room temperature.

Before films preparation, 0.001 g of poly (vinyl alcohol (PVA) was added to each mix. Thin films of CF: PVA and NCC:ZNPs: PVA have been prepared using spin coating method. At speed of $500\ ram/min$ drop of $300\mu l$ was dropped on the rotated glass sub substrate $(25 \times 25)mm$ for (1, 2, and 3) layers, after each layer, the prepared films were heated at 100 °C for 1h.

Structural properties were characterized by XRD instrument, at a scan speed of 4 degree per minute with Cu Kα1 radiation (λ=1.54060 Å) operating at 30 kV and 10 mA. Morphological properties were achieved by analysis of field emission scanning electron microscope (FESEM) and atomic force microscope (AFM). FTIR was characterized to examine changes in the structures of the prepared layers. Gas sensing characterization has been indicated using homemade system by measure the electrical

resistance of the prepared films with nitrogen (N_2), hydrogen (H_2) and ammonia (NH_3) gases exposure by concentrations of (135) ppm with air, as shown in figure (2).

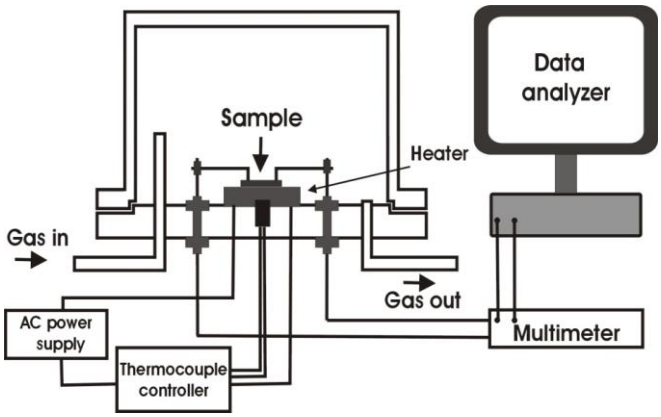

Figure 2. The schematic of the sensing test system used

Gas concentration was obtained with the aid of an equation as follows [28]:

$$Conc(\,ppm) = \; Conc\; gas\; parent(\,ppm)\frac{Flow\; rate\; gas\; parent}{Total\; flow\; rate} \ldots (1)$$

3. Results and Discussion

3.1. SEM and FE- SEM analysis

The prepared CFs made up from palm fronds have been shown a long fibrous shape. These filaments are made of fibers with layer fibrous sheets about 60 nm of thickness consist of nano tapes between 30 nm to 70 nm of width and thickness sequentially, as shown in SEM images, figure (3 A, B and C).

ZNPs clusters appeared clearly in FE-SEM image as individual growths between 20 nm to 240 nm of size, as shown in figure (4-A). Also, figure (4-B) illustrated the aggregation of ZnNPs clusters around NCCs when it was deposited as layers, while, Cellulose fibers (CFs) net has been a as a main structure of the prepared layers, they consist on collections of CFs as rods about 4.5 µm of length and individual ZnONPs , as shown in figure (4-C).

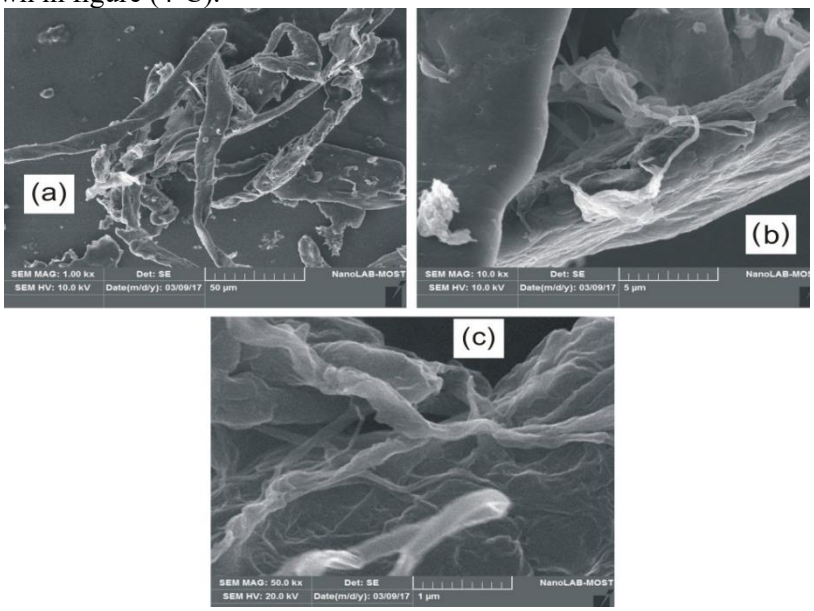

Figure 3. SEM images of the prepared CFs made up from palm fronds

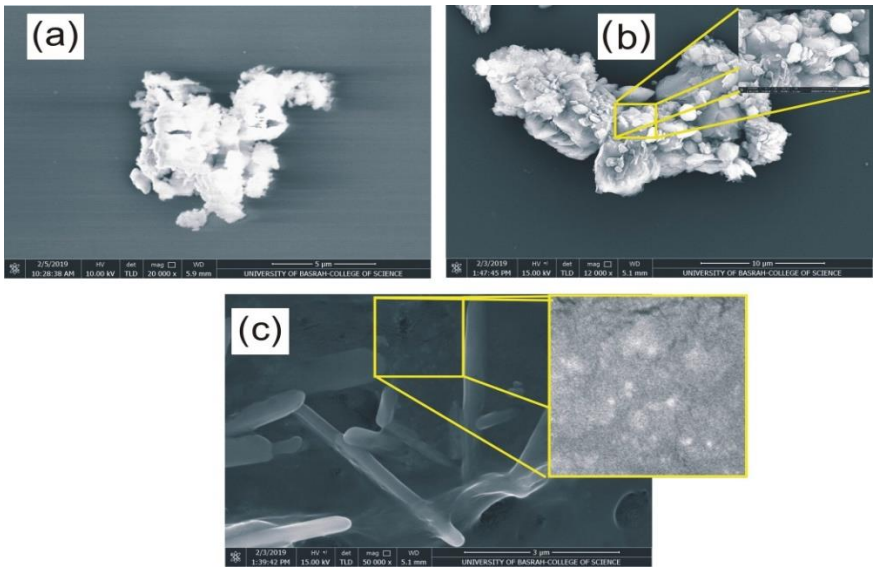

Figure 4. FESEM images of (a) individual growths of ZnONPs, (b) ZnONPs aggregated around CFs and (c) CFs net.

3.2. AFM analysis

The morphological characteristics of NCC layers have been checked using atomic force microscopy (AFM) to observe the superficial shapes. Figure (5) shows images present three- dimensional view of the deposited layers' surface of CFs and NCC:ZNPs. Size and roughness increase with increasing of number of layers. For NCC, the change of size were 56, 94 and 100 nm, while for NCC:ZNPs were 65, 95 and 125 nm. Also roughness changed by 5 nm to 12.2 nm for CF layers, while were 6 nm to 17 nm for NCC:ZNPs.

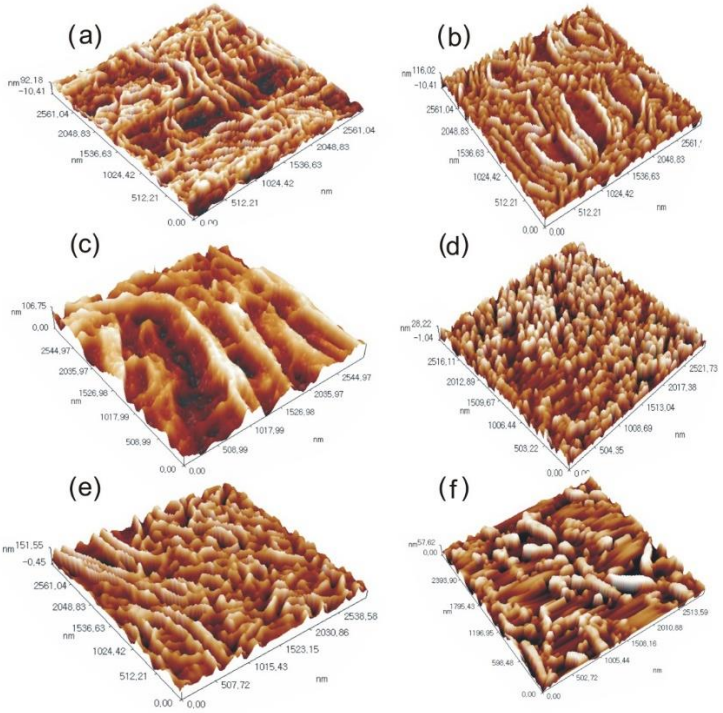

Figure 5. AFM images (a, b, and c) for NCC layers and (d, e, and f) for NCC: ZNPs sequentially.

3.3. XRD analysis

XRD patterns of the prepared layers of CF shown in figure (6). Peaks of [1$\bar{1}$0], [110], [200], and [004] plans of CF crystals shown clearly, in accordance with results of Ismail K. et al.[27] and Mazhar Ul-Islam et al.[29] . Intensities of peaks increased with increasing of the number of layers. In addition, there is shaft and change in the location of peaks due to change in the aggregation of fibers.

Adding of the ZNPs nanoparticles lead to emerge peaks of ZnO for [100], [210], and [200] plans, moreover to peak of bio(2, 4, 6-trimethylphenyl) zinc(II) with [060] plan, while, the spectrum of 3L sample which did not heat has not this peak, as shown in figure (7), this is likely to have occurred due to heating as clear comparing spectra of 3L and 3L without heating, this confirms to bound Zn^{+} with NCC to restrict bonds due to heating.

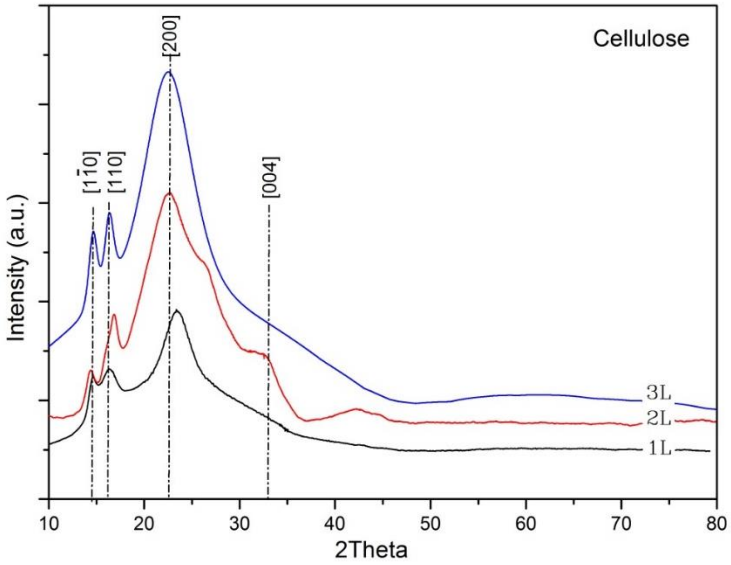

Figure 6. XRD patterns of the prepared films of CF for (1, 2 and 3) layers.

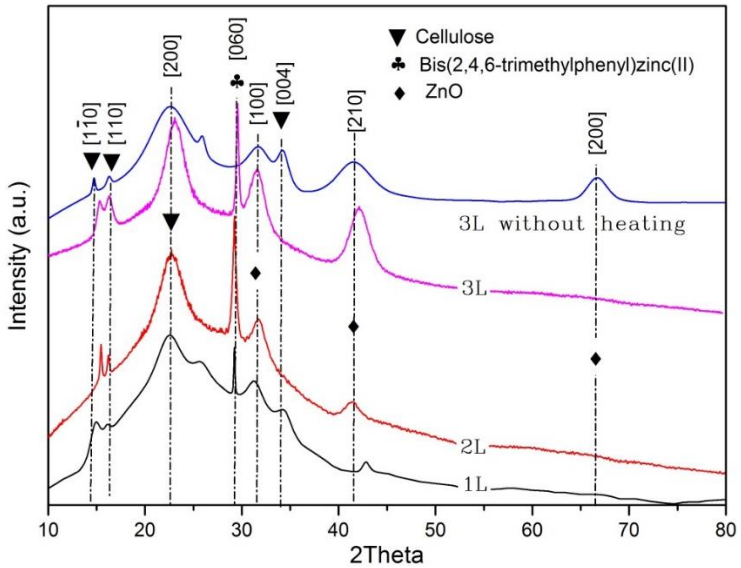

Figure 7. XRD patterns of the prepared films of CF: ZnO for (1, 2 and 3) layers.

The crystallinity indices ($X_{C.I}$)of prepared layers have been calculated using Herman's equation[30];

$$X_{C.I} = \left[\frac{\sum A_{cryst}}{\sum A_{cryst} + \sum A_{amrph}}\right] \times 100\% \quad \ldots\ldots\ldots (2)$$

where A_{cryst} and A_{amrph} are the crystalline area and the amorphous area under the spectrum of XRD respectively. The crystallinity indices of CF ranged from about (59.2 to 82.5) %, whereas were from about (42.3 to 69) % for CF:ZNPs layers. Generally, there is increasing in $X_{C.I}$ with the number of layers were increased in both NCC and NCC:ZNPs films as shown in figure (8). That is contrary to what Han et al reported[31].

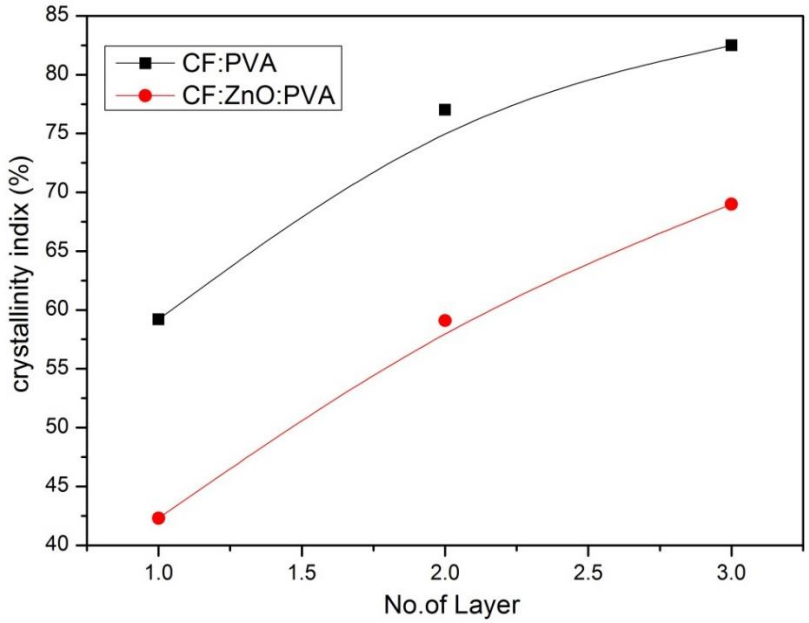

Figure 8. Crystallinity indices of the prepared films of NCC and NCC: ZNPs for (1, 2 and 3) layers.

Whereas the content of the amorphous phase can be given by[32];

$$Y = 1 - X_{C.I} \quad \ldots\ldots \quad (3)$$

3.4. FTIR analysis

Fourier transforms infrared spectra of NCC and NCC: ZNPs were recorded from 400 cm^{-1} to 4000 cm^{-1}, as shown in figure (9). For CF, the stretching characteristic of O-H band shown to 3340 cm^{-1} related carboxylic amine group persons[33]. The peak at 2929 cm^{-1} attributed to the stretching vibration C-H or CH2 related with the methyl hydrogen ring[34], which is shifted to 2876 cm^{-1} after adding of ZNPs. Two peaks at 2376 cm^{-1} and 2321 cm^{-1} respectively have been emerged after add of ZNPs also. The disappearance of C=H which was indicated at 1712 cm^{-1} in the NCC:ZNPs spectrum support the conjugating of ZnO with CF structure. The small peak at 1638 cm^{-1} attributed to the C=O stretching. While, peaks between (1450 and 1260) cm^{-1} indicated to (C=O[14], C-C[34], C-H, and CH_2X (wag)) stretching respectively, which weaken when ZnONPs added lastly, three small peaks shown clearly between 590 cm^{-1} and 452 cm^{-1} in ZNPs spectra attributed to S-S bands which are may be related to the last treatment processes.

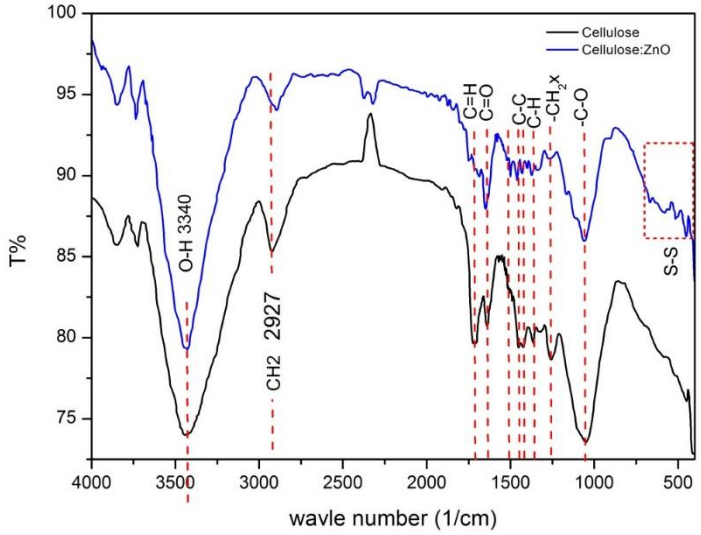

Figure 9. FTIR of the prepared films of CF and CF: ZnONPs.

3.5. Sensing application

Figure 10 illustrated the sensitivity of NCC and NCC: ZNPs sensitivity of N_2, H_2, and NH_3 gases at RT with 135ppm. Both layers showed as good responsive for all gases. Adding of ZNPs leads to enhancement of the sensing of H_2 and NH_3 due to the adsorption of ZNPs of them which leads to increase of the electrical resistance of layer surface. The sensitivity of NCC layers be found at around (21.25, 26 and 68.7) % for NH_3, H_2 and N_2 respectively, whilst, their sensitivity increase with adding of ZNPs by around (40, 26 and 1.4) % for NH_3, H_2 and N_2 respectively. The decreased negligible value in the sensitivity of NCC:ZNPs layers due to N_2 chemical nature as a chemically non-reactive gas[22], that ZnONPs did not enhance the sensory performance for N_2. So, ZNPs did enhance the sensory performance for NH_3 and H_2. Table 1 includes the sensitivity, response and recovery times of CF and NCC:ZNPs sensitivity of N_2, H_2, and NH_3 gases at RT with 135ppm.

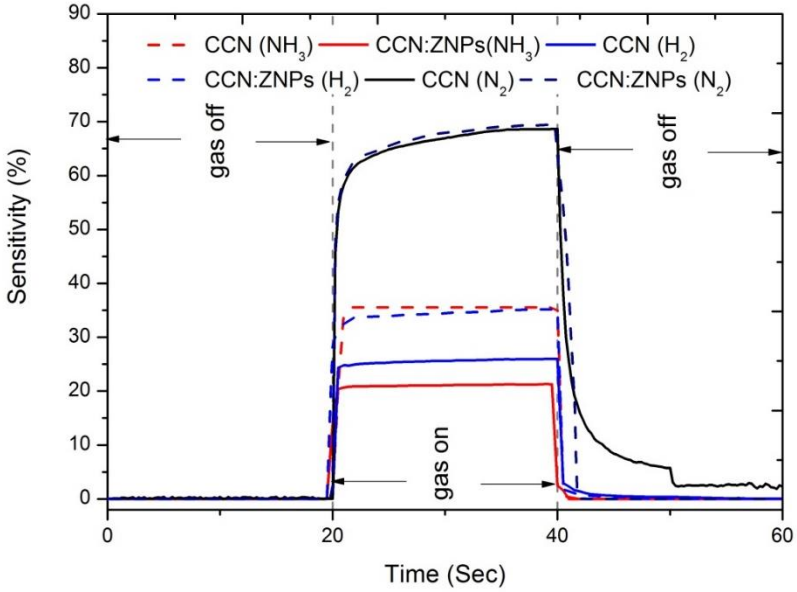

Figure 10. The sensitivity of CF and NCC:ZNPs sensitivity of N2, H2, and NH3 gases at RT with 135ppm.

Table 1. Table 1 includes the sensitivity, response and recovery times of CF and NCC:ZNPs sensitivity of N2, H2, and NH3 gases at RT with 135ppm.

Layer Type	Gas	S%	Res. Time	Rec. Time
NCC	NH3	21.34 ± 0.10	0.40 ± 0.02	0.57 ± 0.01
	H2	25.97 ± 0.08	0.40 ± 0.04	0.70 ± 0.02
	N2	68.68 ± 0.06	2.10 ± 0.06	6.90 ± 0.03
NCC:ZNPs	NH3	35.54 ± 0.09	0.75 ± 0.01	0.70 ± 0.00
	H2	35.18 ± 0.11	0.40 ± 0.07	0.50 ± 0.05
	N2	69.58 ± 0.02	69.58 ± 0.01	69.58 ± 0.08

4. Conclusion

Cellulose is most widespread in nature, safe, and has global economic importance. It can use in wide applications including gas sensors. CFs had the ability to adsorb ZnONPs, and showed nanocrystalline structural. Sensing measurements of proved good devices gas sensitivity for NH3, H2, and N2. Adding of ZnONPs to CF did not effect on the sensitivity of NCC:ZNPs layers because of chemical non activity of N2.

References

[1] E. F. Gaspar, D., S. N. Fernandes, A. G. De Oliveira, J. G. Fernandes, P. Grey, R. V. Pontes, L. Pereira, R. Martins, M. H. Godinho, "Nanocrystalline cellulose applied simultaneously as the gate dielectric and the substrate in flexible field effect transistors," Nanotechnology, vol. 25, no. 9, p. 094008(11), 2014.

[2] C. Salas, T. Nypelö, C. Rodriguez-Abreu, C. Carrillo, and O. J. Rojas, "Nanocellulose properties and applications in colloids and interfaces," Curr. Opin. Colloid Interface Sci., vol. 19, no. 5, pp. 383–396, 2014.

[3] M. A. Hubbe, P. Ferrer, A., Tyagi, Y. Yin, C. Salas, L. Pal, and O. J. Rojas, "Nanocellulose in Thin Films, Coating, and Plies for Packaging Applications: A Review," BioResources, vol. 12, no. 1, pp. 2143–2233, 2017.

[4] R. Sabo, A. Yermakov, C. T. Law, and R. Elhajjar, "Nanocellulose-Enabled Electronics, Energy Harvesting Devices, Smart Materials and Sensors: A Review," J. Renew. Mater., vol. 4, no. 5, pp. 297–312, 2016.

[5] M. Z. Domingo, "Integration of gold nanoparticles (AuNPs) in a nanopaper matrix," Universitat de Girona, 2015.

[6] A. Ali et al., "Zinc impregnated cellulose nanocomposites: Synthesis, characterization and applications," J. Phys. Chem. Solids, vol. 98, pp. 174–182, 2016.

[7] M. Poloju, N. Jayababu, and M. V. Ramana Reddy, "Improved gas sensing performance of Al doped ZnO/CuO nanocomposite based ammonia gas sensor," Mater. Sci. Eng. B Solid-State Mater. Adv. Technol., vol. 227, no. January, pp. 61–67, 2018.

[8] Z. Li et al., "Advances in designs and mechanisms of semiconducting metal oxide nanostructures for high-precision gas sensors operated at room temperature," Mater. Horizons, vol. 6, no. 3, pp. 470–506, 2019.

[9] Z. SV and U. VV, "Facile Sol-gel Synthesis of Metaloxide Nanoparticles in a Cellulose Paper Template," J. Nanomed. Nanotechnol., vol. s8, pp. 8–10, 2017.

[10] M. A. H. Khan, M. V. Rao, and Q. Li, "Recent advances in electrochemical sensors for detecting toxic gases: NO2, SO2 and H2S," Sensors (Switzerland), vol. 19, no. 4, 2019.

[11] J. Ma, W. Zhu, Y. Tian, and Z. Wang, "Preparation of Zinc Oxide-Starch Nanocomposite and Its Application on Coating," Nanoscale Res. Lett., vol. 11, no. 1, p. 200, 2016.

[12] A. Sanmugam, D. Vikraman, S. Venkatesan, and H. J. Park, "Optical and Structural Properties of Solvent Free Synthesized Starch/Chitosan-ZnO Nanocomposites," J. Nanomater., vol. 2017, 2017.

[13] H. U. Ko, S. Mun, S. K. Min, G. W. Kim, and J. Kim, "Fabrication of cellulose ZnO hybrid nanocomposite and its strain sensing behavior," Materials (Basel)., vol. 7, no. 10, pp. 7000–7009, 2014.
[14] M. Shaban, F. Mohamed, and S. Abdallah, "Production and Characterization of Superhydrophobic and Antibacterial Coated Fabrics Utilizing ZnO Nanocatalyst," Sci. Rep., vol. 8, no. 1, pp. 1–15, 2018.
[15] M. Asrofi, H. Abral, A. Kasim, and A. Pratoto, "XRD and FTIR Studies of Nanocrystalline Cellulose from Water Hyacinth (Eichornia crassipes) Fiber," J. Metastable Nanocrystalline Mater., vol. 29, pp. 9–16, 2017.
[16] F. Hruska and S. Plsek, "Gas sensors and their selection," Int. J. Circuits, Syst. Signal Process., vol. 6, no. 5, pp. 350–358, 2012.
[17] S. Pandey, "Highly sensitive and selective chemiresistor gas/vapor sensors based on polyaniline nanocomposite: A comprehensive review," J. Sci. Adv. Mater. Devices, vol. 1, no. 4, pp. 431–453, 2016.
[18] W. B. Harding BE, "Case report of suicide by inhalation of nitrogen gas," Am. J. Forensic Med. Pathol., vol. 29, no. 3, pp. 235–7, 2008.
[19] H. Gu, Z. Wang, and Y. Hu, Hydrogen gas sensors based on semiconductor oxide nanostructures, vol. 12, no. 5. 2012.
[20] G. H. Mhlongo, D. E. Motaung, F. R. Cummings, H. C. Swart, and S. S. Ray, "A highly responsive NH3 sensor based on Pd-loaded ZnO nanoparticles prepared via a chemical precipitation approach," Sci. Rep., vol. 9, no. 1, pp. 1–18, 2019.
[21] V. S. Bhati, M. Hojamberdiev, and M. Kumar, "Enhanced sensing performance of ZnO nanostructures-based gas sensors: A review," Energy Reports, 2019.
[22] P. Shankar and J. Rayappan, "Gas sensing mechanism of metal oxides: The role of ambient atmosphere, type of semiconductor and gases-A review," Sci. Lett. J, vol. 4, no. 4, p. 126, 2015.
[23] M. Strømme, A. Mihranyan, R. Ek, and G. A. Niklasson, "Fractal Dimension of Cellulose Powders Analyzed by Multilayer BET Adsorption of Water and Nitrogen," J. Phys. Chem. B, vol. 107, no. 51, pp. 14378–14382, 2003.
[24] S. Ebrahimiasl and A. Zakaria, "Electrochemical synthesis, characterization and gas sensing properties of hybrid Ppy/CS coated ZnO nanospheres," Int. J. Electrochem. Sci., vol. 11, pp. 9902–9916, 2016.
[25] C. Hsiao and L. Luo, "A Rapid Process for Fabricating Gas Sensors," Sensors, vol. 14, pp. 12219–12232, 2014.
[26] Z. Pang et al., "A room temperature ammonia gas sensor based on cellulose/TiO2/PANI composite nanofibers," Colloids Surfaces A Physicochem. Eng. Asp., vol. 494, pp. 248–255, 2016.
[27] I. K. I. Al-khateeb, S. M. Hussin, and Y. M. Al-obaidi, "Extraction of Cellulose Nano Crystalline from Cotton by Ultrasonic and Its Morphological and Structural Characterization," Int. J. Mater. Chem. Phys., vol. 1, no. 2, pp. 99–109, 2015.
[28] P. M. Perillo and D. F. Rodríguez, "TiO2 Nanotubes Membrane Flexible Sensor for Low-Temperature H2S Detection," Chemosensors, vol. 4, no. 3, p. 15, 2016.
[29] M. Ul-Islam, W. A. Khattak, M. W. Ullah, S. Khan, and J. K. Park, "Synthesis of regenerated bacterial cellulose-zinc oxide nanocomposite films for biomedical applications," Cellulose, vol. 21, no. 1, pp. 433–447, 2014.
[30] M. Poletto, H. L. Ornaghi Júnior, and A. J. Zattera, "Native cellulose: Structure, characterization and thermal properties," Materials (Basel)., vol. 7, no. 9, pp. 6105–6119, 2014.
[31] J. Han, C. Zhou, Y. Wu, F. Liu, and Q. Wu, "Self-assembling behavior of cellulose nanoparticles during freeze-drying: Effect of suspension concentration, particle size, crystal structure, and surface charge," Biomacromolecules, vol. 14, no. 5, pp. 1529–1540, 2013.
[32] M. Ioelovich and A. Leykin, "Study of sorption properties of cellulose and its derivatives,"

BioResources, vol. 6, no. 1, pp. 178–195, 2011.

[33] A. Sanmugam, D. Vikraman, S. Venkatesan, and H. J. Park, "Optical and Structural Properties of Solvent Free Synthesized Starch / Chitosan-ZnO Nanocomposites," J. Nanomater., vol. 2017, p. 8, 2017.

[34] D. Tanasa, N. Vrinceanu, A. Nistor, Brinza F., Chicet, D. and Broasca G. (2012). "Zinc oxide-linen fibrous composites : morphological , structural , chemical and humidity adsorptive attributes," Text. Res. J., vol. 82, no. 8, pp. 832–844.